Article:
Elf, S, Abdelfattah, NS, Chen, E orcid.org/0000-0003-0742-9734 et al. (13 more authors) (2016) Mutant Calreticulin Requires Both Its Mutant C-terminus and the Thrombopoietin Receptor for Oncogenic Transformation. Cancer Discovery, 6 (4). pp. 368-381. ISSN 2159-8274

https://doi.org/10.1158/2159-8290.CD-15-1434

Mutant calreticulin requires both its mutant C-terminus and the thrombopoietin receptor for oncogenic transformation

Shannon Elf[1,6], Nouran S. Abdelfattah[1,6], Edwin Chen[1,6], Javier Perales-Patón[2], Emily A. Rosen[1], Amy Ko[1], Fabian Peisker[1], Natalie Florescu[1], Silvia Giannini[1], Ofir Wolach[1], Elizabeth A. Morgan[3], Zuzana Tothova[1,4,5], Julie-Aurore Losman[4], Rebekka K. Schneider[1], Fatima Al-Shahrour[2], Ann Mullally[1,4,5]

Correspondence:
amullally@partners.org
Phone: (617) 355-9002
Fax: (617) 355-9153

1, Blackfan Circle
Karp Building, Room 5.125
Boston, MA 02115

RUNNING TITLE
Mutant CALR requires its C-terminus and MPL to transform

Conflict-of-interest disclosure: The authors declare no competing financial interests.

[1] Division of Hematology, Department of Medicine, Brigham and Women's Hospital, Harvard Medical School, Boston, Massachusetts 02115, USA.
[2] Translational Bioinformatics Unit, Clinical Research Programme, Spanish National Cancer Research Centre (CNIO), Madrid, Spain.
[3] Department of Pathology, Brigham and Women's Hospital, Harvard Medical School, Boston, Massachusetts 02115, USA.
[4] Broad Institute, Cambridge, Massachusetts 02142, USA.
[5] Dana-Farber Cancer Institute, Harvard Medical School, Boston, MA 02115, USA.
[6] These authors contributed equally to this work.

ABSTRACT

Somatic mutations in calreticulin (*CALR*) are present in approximately 40% of patients with myeloproliferative neoplasms (MPN) but the mechanism by which mutant CALR is oncogenic remains unclear. Here, we demonstrate that expression of mutant CALR alone is sufficient to engender MPN in mice and recapitulates the disease phenotype of *CALR*-mutant MPN patients. We further show that the thrombopoietin receptor, MPL is required for mutant CALR-driven transformation through JAK-STAT pathway activation, thus rendering mutant CALR-transformed hematopoietic cells sensitive to JAK2 inhibition. Finally, we demonstrate that the oncogenicity of mutant CALR is dependent on the positive electrostatic charge of the C-terminus of the mutant protein, which is necessary for physical interaction between mutant CALR and MPL. Together, our findings elucidate a novel paradigm of cancer pathogenesis and reveal how *CALR* mutations induce MPN.

STATEMENT OF SIGNIFICANCE

The mechanism by which calreticulin (*CALR)* mutations induce myeloproliferative neoplasms (MPN) remains unknown. In this report, we show that the positive charge of the CALR mutant C-terminus is necessary to transform hematopoietic cells by enabling binding between mutant CALR and the thrombopoietin receptor MPL.

INTRODUCTION

Myeloproliferative neoplasms (MPN) are clonal disorders of hematopoiesis arising in the hematopoietic stem cell (HSC) compartment and characterized by an excess production of mature blood cells of the myeloid lineage (1, 2). BCR-ABL negative MPN comprise three distinct diseases, polycythemia vera (PV), essential thrombocythemia (ET) and myelofibrosis (MF). PV is characterized by myeloid hyperplasia and increased red cell mass; ET, by megakaryocytic hyperplasia and increased platelet counts; and MF, by megakaryocytic hyperplasia in conjunction with bone marrow fibrosis. These disorders share a common molecular basis unified by aberrant cytokine signaling. A V617F activating mutation in the non-receptor tyrosine kinase JAK2 (JAK2V617F) results in hyperactive JAK-STAT signaling downstream of multiple hematopoietic cytokine receptors, including the erythropoietin receptor (EPOR) and thrombopoietin receptor (MPL) (3-6) and is present in ~95% of PV patients and 50-60% of ET and MF patients. Activating mutations in MPL have also been detected in 1-5% of ET and MF patients (7) (8), and negative regulators of JAK-STAT signaling such as LNK (9), c-CBL (10, 11) or SOCS (12) are also somatically inactivated at low frequency in MPN patients.

Recent whole exome sequencing studies have revealed that the majority of the remaining JAK2-unmutated and MPL-unmutated ET and MF patients harbor somatic mutations within the gene, *CALR* (13, 14). *CALR* encodes a Ca^{2+} binding chaperone protein, calreticulin that localizes primarily to the endoplasmic reticulum (ER) and regulates protein folding quality control pathways (15). The wild-type CALR protein comprises three protein domains: (i) a conserved N domain, which contains residues that regulate CALR chaperone activity, (ii) a central P domain, which contains a lectin-like chaperone site, and (iii) a C-domain, which includes a string of negatively-charged

amino acid residues responsible for Ca^{2+} buffering and a C-terminus ER retention signal (KDEL) (16). More than thirty different *CALR* mutations have been identified in MPN patients, all of which are small insertions and/or deletions (indels) within exon 9 that lead to a one base-pair (+1 bp) reading frameshift and the generation of a mutant-specific 36 amino acid C-terminal tail. The mutant-specific CALR C-terminal tail lacks the KDEL ER-retention signal and contains an abundance of positively-charged amino acids (13). The relevance of these features to the oncogenicity of mutant CALR remains unclear.

In this study, we dissect the functional and biochemical activity of the most common *CALR* mutation observed in MPN patients (i.e. p.L367fs*46 which results in a 52bp deletion) and report three major advances in understanding the pathogenesis of *CALR*-mutant MPN: (i) we provide an explanation for the megakaryocyte lineage-specific clinical phenotype of *CALR*-mutant MPN, (ii) we delineate the oncogenic role of the CALR mutant-specific C-terminus in the pathogenesis of *CALR*-mutant MPN, and (iii) we provide a biological basis for the observation that JAK2V617F and *CALR* mutations are typically mutually exclusive in MPN patients.

RESULTS

Mutant CALR is sufficient to engender an MPN phenotype in mice

The role of BCR-ABL (17, 18), JAK2V617F (19-22) and MPLW515L (7) as *bona fide* MPN driver mutations was demonstrated based on their ability to induce MPN phenotypes in mice (23). However, equivalent data for *CALR* mutations are currently lacking. In order to test whether expression of mutant CALR alone could similarly induce an MPN phenotype in mice, we performed bone marrow transplantation (BMT)

experiments whereby c-Kit-enriched primary mouse bone marrow cells were transduced with retroviruses expressing either an empty vector (EV), a wild-type human CALR cDNA ($CALR^{WT}$) or a mutant human CALR cDNA ($CALR^{MUT}$), and transplanted the cells into lethally irradiated recipient mice (Figure 1A). The specific *CALR* mutation used throughout this study was the 52bp deletion.

Donor-derived chimerism for both $CALR^{WT}$- and $CALR^{MUT}$-expressing cells decreased relative to EV-expressing cells, which may indicate a cytotoxic effect associated with CALR over-expression (Figure S1A). However, by 16-weeks post-transplantation, mice transplanted with cells expressing $CALR^{MUT}$ (but not $CALR^{WT}$ or EV) had developed an MPN phenotype reminiscent of ET, characterized by isolated thrombocytosis (Figure 1B) and megakaryocytic hyperplasia (Figure 1C, D, Figure S1B). The megakaryocytes in $CALR^{MUT}$ mice were markedly enlarged with hyperlobulated nuclei and emperipolesis, consistent with an MPN phenotype (Figure 1C). Given the megakaryocyte lineage-specific phenotype of $CALR^{MUT}$-expressing mice, we next assessed CALR expression in primary MPN bone marrow samples using immunohistochemical analysis. Consistent with recent reports (24, 25), we found that CALR is highly expressed in megakaryocytic lineage cells and in immature myeloid cells in the bone marrow of *CALR*-mutant MPN patients, with little or no CALR expression observed in erythroid lineage cells or in mature myeloid cells (Figure S1C).

We also performed flow cytometric analysis to characterize the stem and progenitor cell compartment of the bone marrow in the transplanted mice. We observed a modest expansion of the Lin−Sca-1+c-Kit+ (LSK) compartment, which is enriched for hematopoietic stem cell (HSC) activity, in $CALR^{MUT}$ mice relative to EV mice ($p=0.02$) or $CALR^{WT}$ mice ($p=0.03$) (Figure S1D). In contrast, no significant expansion of the

Lin−Sca-1−c-Kit+ (LK) myeloid progenitor cell compartment was observed (Figure S1D). Together, these data indicate that over-expression of mutant CALR alone is sufficient to engender an MPN phenotype in mice and the disease phenotype that ensues closely recapitulates the clinical features observed in *CALR*-mutant MPN patients.

MPL is required for mutant CALR-mediated cellular transformation

The megakaryocyte lineage-specific phenotype of *CALR*-mutant MPN prompted us to investigate the role of MPL in disease pathogenesis. For this, we employed a standard Ba/F3 cellular transformation assay. Ba/F3 cells are a murine interleukin 3 (IL-3)-dependent hematopoietic cell line that can be rendered IL-3 independent upon ectopic expression of certain oncogenes such as BCR-ABL (26). In the case of JAK2V617F, however, this transformation requires co-expression of a type I cytokine receptor such as the erythropoietin receptor (EPOR) or MPL (27). We found that $CALR^{WT}$ or $CALR^{MUT}$ were both incapable of transforming parental Ba/F3 cells to IL-3 independence (Figure 2A). However, we found that $CALR^{MUT}$ (but not $CALR^{WT}$) was able to successfully transform Ba/F3 cells to IL-3 independence upon co-expression of MPL (Figure 2B). This dependence on MPL was specific, as $CALR^{MUT}$ was incapable of transforming cells expressing other type I hematopoietic cytokine receptors, such as the EPOR and the granulocyte-colony stimulating factor receptor (G-CSFR) to IL-3 independence (Figures 2C, D). Similarly, we observed that $CALR^{MUT}$ was able to transform human megakaryocytic UT-7 cells (28) to GM-CSF-independence when MPL (but not EPOR or G-CSFR) was stably expressed, demonstrating that this effect is not restricted to Ba/F3 cells (Figure 2E - G). Of note, Jak2V617F indiscriminately transformed all type I cytokine receptor-expressing Ba/F3 cells, pointing to an important distinction between the transforming requirements of JAK2V617F and mutant CALR (Figure 2B - D).

Introduction of +1 bp frameshift mutations into the endogenous *Calr* locus is sufficient to confer oncogenic activity to Calr

To confirm the transforming capacity of mutant Calr when expressed at physiological levels, we employed CRISPR/Cas9 gene editing (29). We first stably expressed Cas9 in parental Ba/F3, Ba/F3-MPL, Ba/F3-EPOR and Ba/F3-G-CSFR cells, then infected each cell line with a small guide RNA (sgRNA) targeting exon 9 of *Calr*, in the region where the 52 bp deletion occurs in *CALR*-mutant MPN patients (Figure S2). To ensure that the observed effects were due to on-target gene editing we performed separate infections using two distinct sgRNAs (m1 or m2) each targeting exon 9 of *Calr* and compared our findings to cells infected with a scramble sgRNA control (Figure 3A – D). We observed IL-3-independent outgrowth of *Calr*-targeted Ba/F3-MPL-Cas9 cells (Figure 3B) but not *Calr*-targeted parental Ba/F3-Cas9 cells (Figure 3A) or *Calr*-targeted Ba/F3-Cas9 cells overexpressing EPOR (Figure 3C) or G-CSFR (Figure 3D). To confirm that IL-3 independent growth in *Calr*-targeted Ba/F3-MPL-Cas9 cells was a result of an on-target event, we harvested cells 8 days post IL-3 withdrawal and extracted genomic DNA. We then PCR amplified a 422 bp region spanning the target site, performed sub-cloning of PCR amplicons and sequenced 30 individual clones. Out of 13 sub-clones from m1 *Calr*-targeted Ba/F3-MPL-Cas9 cells, 11 were found to contain indels that led to +1 bp frameshift mutations. For m2 *Calr*-targeted Ba/F3-MPL-Cas9 cells, 10 sub-clones out of 17 were found to contain indels that led to +1 bp frameshifts, and 3 of the 10 showed a 52 bp deletion within exon 9 (Figure 3E). These data confirm that MPL is required for mutant Calr to transform Ba/F3 cells and demonstrate that introduction of a +1 bp frameshift to the endogenous *Calr* locus is sufficient to confer oncogenic activity to Calr. Furthermore, the sequencing data (Figure 3E) suggests that the introduction of

heterozygous +1 bp frameshift mutations to the endogenous *Calr* locus is sufficient to transform Ba/F3-MPL cells, consistent with the observation that *CALR* mutations are typically heterozygous in MPN patients (13, 14).

Mutant CALR activates the JAK-STAT signaling axis downstream of MPL

We next performed whole transcriptome RNA-sequencing to identify gene expression changes associated with mutant CALR-mediated transformation. We found that $CALR^{MUT}$-transformed Ba/F3-MPL cells grown in the absence of IL-3 for 24 hours display strong enrichment of Stat5 (30) (31) and Stat3 (31) (32) gene expression signatures when compared to cells overexpressing $CALR^{WT}$ (Figure 4A, Figure S3A, Supplemental Table 1). In consonance, immunoblotting revealed activation of MPL, Jak2, Stat5 and Stat3 in $CALR^{MUT}$-transformed Ba/F3-MPL cells that were starved of IL-3 for 24 hours, but no evidence of Stat activation in IL-3 starved parental Ba/F3, Ba/F3-EPOR, or Ba/F3-G-CSFR cells expressing $CALR^{MUT}$ (Figure 4B-C). We also observed activation of STAT5 in UT-7-MPL cells transformed to GM-CSF independence by ectopic expression of $CALR^{MUT}$ (Figure S3B) and activation of Stat5 and Stat3 in Ba/F3-MPL cells transformed to IL-3 independence through the introduction of +1 bp frameshift mutations to the endogenous *Calr* locus by CRISPR/Cas9 gene editing (Figure S3C).

Mutant CALR-transformed hematopoietic cells are sensitive to JAK2 inhibition

Given the increased Jak-Stat activity in $CALR^{MUT}$-transformed Ba/F3-MPL cells, we next evaluated the sensitivity of these cells to Jak2 inhibition. We performed shRNA-mediated knockdown of Jak2 (using two separate shRNAs) and found that Jak2 knockdown significantly decreased the proliferative rate of $CALR^{MUT}$-transformed Ba/F3-MPL cells

(growing in the absence if IL-3) relative to a non-targeting shRNA control (p=0.0001, Figure 5A). Moreover, we found that the differential activation of Stat3 in these cells was abrogated by treatment with the JAK1/2 inhibitor, INCB018424 (ruxolitinib) (33) (Figure 5B). Concordant with this, genes downregulated in JAK2 inhibitor signatures were enriched in Ba/F3-MPL cells expressing $CALR^{MUT}$ as compared to $CALR^{WT}$-expressing Ba/F3 MPL cells (Figure 5C). Together, these data demonstrate that $CALR^{MUT}$ transforms cells through activation of the JAK-STAT signaling axis downstream of MPL and that Ba/F3-MPL cells transformed by $CALR^{MUT}$ are sensitive to Jak2 inhibition.

The CALR mutant C-terminus is necessary but not sufficient for transformation

We next sought to understand the biochemical basis by which the mutant C-terminus of $CALR^{MUT}$ contributes to transformation. To define the specific domains within $CALR^{MUT}$ necessary for oncogenic transformation, we generated a panel of mutated versions of $CALR^{MUT}$ and systematically assessed their ability to transform Ba/F3-MPL cells.

We began by generating a series of CALR domain mutants. We first generated N domain and P domain versions of CALR. The N domain cDNA encodes the first 197 shared amino acids between WT and mutant CALR while the P domain cDNA encodes the middle 111 shared amino acids between WT and mutant CALR. We then generated $CALR^{WT}$ C domain and $CALR^{MUT}$ C domain versions of CALR (C $domain^{WT}$ and C $domain^{MUT}$ respectively) that differ in the terminal 36 amino acids that distinguish mutant CALR from WT CALR (Figure 6A). We found that ectopic expression of the N, P, or C $domain^{WT}$ domain-only versions of CALR alone were incapable of transforming Ba/F3-MPL cells to IL-3 independence (Figure 6B). Moreover, we found that ectopic expression of the $CALR^{MUT}$ C domain alone was also unable to transform Ba/F3-MPL cells to IL-3

independence (Figure 6B). Together, these data indicate that the CALR mutant C-terminus is necessary but alone is not sufficient for transformation (Figure 6A - B).

We next focused on altering the full-length $CALR^{MUT}$ protein. One of the most prominent features of *CALR* mutations is that they all result in loss of the terminal KDEL motif necessary for ER retention. We therefore tested whether loss of this sequence alone renders CALR an oncogene. We found that only removing the KDEL sequence from $CALR^{WT}$ did not lead to transformation of Ba/F3-MPL cells (Figure 6C). This finding suggests that the mutant CALR C-terminus does not exert its oncogenic activity solely through CALR mislocalization but rather the novel mutant C-terminus likely imparts a gain-of-function, a conclusion consistent with an absence of MPN patients harboring +2 frameshifts which causes a premature stop codon (13).

Structure-function analysis of mutant CALR uncovers a critical oncogenic role for the positive electrostatic charge of the mutant C-terminus

Having demonstrated that the introduction of +1 bp frameshift mutations to the endogenous *Calr* locus is sufficient to transform Ba/F3-MPL-Cas9 cells (Figure 3B) we noted that differences exist between human mutant CALR and mouse mutant Calr protein sequences (Figure S4A-B). This suggested to us that the oncogenic properties of the CALR mutant C-terminus may not reside within a specific residue or sequence of residues but rather reflect a shared property of the neo-morphic C-terminal tail of human mutant CALR and mouse mutant Calr. To test this hypothesis, we first synthesized a series of $CALR^{MUT}$ C-terminus sequence-mutants in which blocks of 8-10 amino acids of the mutant C-terminus were individually deleted ($CALR^{MUT}\Delta$0-8, $CALR^{MUT}\Delta$9-18, $CALR^{MUT}\Delta$19-26, $CALR^{MUT}\Delta$27-36) (Figure 6A). We found that all four $CALR^{MUT}$ C-

terminus sequence-mutants were capable of transforming Ba/F3-MPL cells with equal efficacy (Figure 6D). These data are consistent with our hypothesis that the transforming activity of mutant CALR is not contained within specific residues within the $CALR^{MUT}$ C-terminus.

MPN-associated *CALR* mutations replace a group of negatively-charged amino acids in the C-terminus of $CALR^{WT}$ protein with a surplus of positively-charged amino acids (most often lysine (K) and arginine(R)) in the C-terminus of $CALR^{MUT}$ protein (13). We therefore next hypothesized that the shared oncogenic property of the neo-morphic C-terminal tail of human mutant CALR and mouse mutant Calr may relate to the positive electrostatic charge of the mutant C-terminus. To test this hypothesis we designed a $CALR^{MUT}$ C-terminus in which every K and R residue in the C-terminus of mutant CALR was replaced with a neutral glycine (G) ($CALR^{MUT}$-neutral, Figure 6E). As a control, we replaced every non-K and non-R residue with a glycine ($CALR^{MUT}$-positive, Figure 6E). Remarkably, expression of $CALR^{MUT}$-positive retained the ability to transform Ba/F3-MPL cells to IL-3 independence (Figure 6E), despite 18 of 36 amino acids within the C-terminus being altered to glycine and the majority of the C-terminus being comprised of only 3 different amino acids. In contrast, the $CALR^{MUT}$-neutral was incapable of transforming BaF3-MPL cells to IL-3 independence (Figure 6E).

In aggregate, these findings reveal an essential requirement for the positive electrostatic charge of the $CALR^{MUT}$ C-terminus in mediating the transforming activity of $CALR^{MUT}$, while revealing a striking degeneracy with regard to the sequence requirements.

Mutant CALR binds to MPL and this interaction correlates with the transforming capacity of mutant CALR

Given the absolute requirement for MPL in $CALR^{MUT}$-mediated transformation, we hypothesized that MPL and $CALR^{MUT}$ may physically interact. To test this hypothesis, we performed FLAG-immunoprecipitation assays in 293T cells co-transfected with MPL and FLAG-tagged CALR variants. In support of the Ba/F3 transformation assay results, we found that compared to $CALR^{WT}$, $CALR^{MUT}$ displayed differential binding to MPL (Figure 7A), but not to EPOR (Figure 7B) or G-CSFR (Figures 7C). We also found increased binding between MPL and mutant Calr (as compared to wild-type Calr) in Ba/F3-MPL-Cas9 cells targeted with CRISPR Cas9 to engender endogenous level mutant Calr expression (Figure S5), demonstrating that this differential interaction is not as a result of over-expressing mutant CALR. Moreover, expression of the mutant C-terminus alone was not sufficient to mediate binding in 293T cells (Figure 7D), suggesting that the tertiary structure of $CALR^{MUT}$ is important for physical interaction with MPL.

Given the essential requirement for the positive electrostatic charge of the $CALR^{MUT}$ C-terminus in $CALR^{MUT}$-mediated transformation, we next tested the ability of the $CALR^{MUT}$ charge variants described in Figure 6E to bind to MPL. We found that binding of $CALR^{MUT}$-neutral to MPL was markedly attenuated as compared to the binding of full-length $CALR^{MUT}$ to MPL, and strikingly that the $CALR^{MUT}$-positive retained the ability to bind MPL (Figure 7E). These findings are in consonance with the Ba/F3 transformation assay results, where $CALR^{MUT}$-neutral does not transform Ba/F3-MPL cells but $CALR^{MUT}$-positive does (Figure 6E).

Taken together these findings reveal a specific physical interaction between MPL and mutant CALR and demonstrate a correlation between the binding of mutant CALR to

MPL and the transforming activity of mutant CALR. In aggregate, our findings suggest that binding of mutant CALR to MPL is required for cellular transformation.

DISCUSSION

The identification of recurrent mutations in *CALR* in MPN is among the most unexpected findings from recent whole exome studies in myeloid malignancies (13, 14). CALR, an ER chaperone protein that normally functions to bind misfolded proteins in the ER and prevent their export to the Golgi (34), had never previously been found to be mutated in cancer or to be associated with hematological disorders.

The presence of recurrent mutations in *CALR* suggests a key pathogenic role for mutant CALR in MPN (13, 14). Our murine BMT data demonstrates that mutant CALR *alone* is sufficient to induce an MPN phenotype *in vivo* and supports the proposition that *CALR* mutations are driver mutations in MPN. These data accord with a recent study, which also used a retroviral BMT mouse model of the CALR 52bp deletion, and observed a similar MPN phenotype (thrombocytosis and megakaryocytic hyperplasia), in addition to the development of myelofibrosis at six months or more post transplantation (35). A central role for mutant CALR in early MPN ontogeny is also consistent with clinical sequencing studies showing that *CALR* mutations are typically mutually exclusive with the other MPN driver mutations (such as JAK2V617F and MPLW515L). Moreover, *CALR* mutations are detectable in the long-term hematopoietic stem cell compartment (13, 14), and clonal analysis of *CALR*-mutated patient samples has shown that *CALR* mutations frequently reside in the earliest detectable phylogenetic node (14).

Our data reveals an essential and specific role for MPL in mutant CALR-mediated cellular transformation in multiple experimental contexts. Firstly, we found that ectopic expression of mutant CALR in Ba/F3 hematopoietic cells requires co-expression of MPL for transformation, a finding also demonstrated in recent reports (35, 36). Importantly, our data further demonstrates a specific requirement for MPL under conditions of endogenous level mutant Calr expression (following CRISPR/Cas9 gene editing in Ba/F3 cells) and in human cytokine-dependent megakaryocytic cells (following lenti-viral delivery in UT-7 cells), which more closely recapitulate *CALR*-mutant MPN. The specificity of the dependence on MPL is in striking contrast to Jak2V617F, which is more agnostic with respect to cytokine receptor co-expression requirements (27, 37). These differences in cytokine receptor requirements align well with how *CALR* and *JAK2* mutations are distributed within the MPN subtypes. *CALR* mutations are restricted to ET and MF (38, 39), which exhibit a megakaryocyte predominant disease phenotype and are not found in PV, where the defining clinical feature is erythrocytosis; JAK2V617F mutations, on the other hand, are found in all three MPN subtypes and JAK2-mutant MPN typically display leukocytosis, erythrocytosis and thrombocytosis. The high degree of cytokine receptor specificity for mutant CALR is likely to relate physical interaction between mutant CALR and MPL but not with other cytokine receptors such as EPOR (discussed below).

Consistent with the mutual exclusivity of *CALR* and *JAK2* mutations in MPN, we observed evidence of increased Jak-Stat signaling in $CALR^{MUT}$-transformed Ba/F3-MPL cells, which we found to be susceptible to genetic and pharmacological inhibition of Jak2 signaling. These findings accord with a recent microarray gene expression analysis which similarly depicts increased JAK-STAT pathway activation in *CALR*-mutant primary MPN granulocytes (40), and with a recent case report describing two *CALR*-mutant MPN

patients who demonstrated clinical responses to the JAK2 inhibitor, fedratinib (41). The clonal selectivity of JAK2 inhibitors for *CALR*-mutant cells in MPN remains to be determined but the on-target toxicity of JAK2 inhibitors (e.g. anemia) is likely to be an issue in the treatment of *CALR*-mutant MPN just as it is in the treatment of *JAK2*-mutant MPN (42), suggesting that novel approaches aimed at preferentially targeting *CALR*-mutant cells in MPN will be needed. A recent study demonstrated the use of non-signaling diabodies to re-orient the EPOR into an inactive dimer topology and thus inhibit the erythropoietin-independent but EPOR-dependent proliferation of primary JAK2V617F-mutant erythroid precursor cells *in vitro* (43). Analogous strategies to inhibit MPL signaling may be a viable strategy to selectively target *CALR*-mutant cells in MPN.

The observation that over 30 disparate mutations all generate the same novel C-terminal peptide tail strongly suggests that *CALR* mutations are gain-of-function or that they confer a neo-morphic function on mutant CALR, with the mutant C-terminus playing a critical oncogenic role. Concordant with this, a recent study reported that over-expression of a CALR mutant in which the entire exon 9 was deleted did not induce MPN in mice (35). Through extensive mutagenesis-based structure-function analysis, our data reveal some novel insights into the role the C-terminus of mutant CALR plays in oncogenesis. Our data proposes a model whereby the oncogenic activity of mutant CALR is not encoded within a specific sequence of the mutant CALR C-terminal tail. Rather, our data demonstrates a role for the positive electrostatic charge of the mutant C-terminus in influencing the ability of mutant CALR to physically associate with MPL, thus facilitating transformation. This model poses two unanswered questions: (1) How does the mutant CALR C-terminus favor MPL binding over other type 1 cytokine receptors? (2) How does this interaction activate JAK-STAT signaling? One possible explanation is that mutant CALR exhibits a different tertiary structure than wild-type

CALR, thus facilitating a specific interaction with MPL. It is also possible that the diminished calcium sequestration capacity of mutant CALR due to loss of the negatively charged amino acids (44) may stabilize MPL association. A recent report showed that a glycosylation site within the extra-cellular domain of MPL is required for mutant CALR-mediated transformation *in vitro,* suggesting that MPL glycosylation influences its ability to interact with mutant CALR (36). Future studies aimed at further addressing these questions are warranted.

In conclusion, our data provide insights into the molecular mechanism by which mutant CALR transforms hematopoietic cells. Specifically, we uncover an essential requirement for MPL in mutant CALR-mediated transformation. We further show that the oncogenicity of mutant CALR is dependent on the positive electrostatic charge of the C-terminus of the mutant protein, which promotes physical interaction with MPL. Together, our findings elucidate a novel paradigm of cancer pathogenesis and help explain how *CALR* mutations drive the development of MPN.

METHODS

Cell Lines. 293T cells were obtained from American Type Culture Collection (ATCC) in 2011 and their identity was authenticated by Short Tandem Repeat (STR) profiling. Ba/F3 cells and UT-7 cells were purchased from German Collection of Microorganisms and Cell Cultures (DSMZ) in 2014 and were not further authenticated. All cell lines were intermittently tested for mycoplasma.

Generation of Type I Cytokine Receptor-Expressing Cell Lines. Type I cytokine receptor-expressing Ba/F3 and UT-7 cell lines were generated by retroviral transduction. In brief, retroviral supernatants were generated by co-transfection of pMSCV-hygro-hMPL, pMSCV-neo-hEPOR, or pMSCV-neo-hG-CSFR with packaging plasmid in 293T cells. Viral supernatants were collected 24 and 48 hours post-transfection. Ba/F3 or UT-7 cells were subjected to spin infection with viral supernatants, followed by 7 days of antibiotic selection. CALR variant lentiviral supernatants were generated by co-transfection of LeGO-iV2 empty vector, LeGO-iV2-CALR wild type, LeGO-iV2-52 bp deletion, or pMSCV-IRES-GFP-Jak2V617F with packaging plasmids in 293T cells. Viral supernatants were collected 24 and 48 hours post-transfection. Stable Ba/F3 and UT-7 lines stably expressing type I cytokine receptors were then subjected to spin infection with CALR variant lentiviral supernatants. 48 hours after spin infection, cells were sorted for GFP expression using a BD FACSAria cell sorter (BD Biosciences).

Generation of Jak2-deficient Ba/F3-MPL Cell Lines. Stable knockdown of endogenous Jak2 in Ba/F3-MPL cells was achieved using a pLKO.1-based lentiviral vector shRNA construct targeting Jak2 (shJak2 #1 5'-CCAACATTACAGAGGCATAAT-3'; shJak2 #2 5' CGTGGAATTTATGCGAATGAT-3') or control non-targeting shRNA against Luciferase

(shLuc 5'-GCTGAGTACTTCGAAATGTCC-3'). The lentiviral backbone vector and packaging plasmids were transfected into 293T cells and the viral supernatant was harvested 24 and 48 hours later. Ba/F3-MPL cells overexpressing $CALR^{MUT}$ were spin infected with lentiviral supernatants as indicated, then subjected to puromycin selection for 7 days.

Ba/F3 and UT-7 Cell Growth Assays. Sorted and exponentially growing Ba/F3 or UT-7 cells were washed four times with PBS and seeded in triplicate at $1x10^5$ cells/mL in RPMI 1640 medium supplemented with 10% FBS and 5% penicillin/streptomycin in the presence or absence of cytokine for indicated time points. Living cells were counted at each time point using a Beckman Coulter VI-Cell XR Cell Viability Analyzer (Beckman Coulter, Fullerton, CA).

CRISPR/Cas9 gene editing. Indel mutations targeting exon 9 of the endogenous *Calr* locus (focused on the region of the 52 bp deletion found in MPN patients) were introduced to Ba/F3 cells using CRISPR/Cas9 gene editing. Stable expression of the codon optimized *Streptococcus pyogenes* Cas9 in parental Ba/F3 cells and Ba/F3 cells overexpressing hMPL, hEPOR or hG-CSFR was achieved by lentiviral transduction of pLX_TRC311-Cas9 (29) and selected with 5μg/ml blasticidin. In brief, lentiviral supernatants were generated by co-transfection of pLX_TRC311-Cas9 with packaging plasmid in 293T cells. Viral supernatants were collected 24 hours post-transfection. Ba/F3 cells were subjected to spin infection with viral supernatants, followed by 9 days of antibiotic selection. Cas9 activity was confirmed using a reporter assay (29). sgRNAs targeting exon 9 of *Calr* were designed using the Broad Institute cleavage efficiency predictor and off-target scores (Supplementary table 2) were obtained from the MIT Optimized CRISPR Design website (29). For sgRNA cloning, the

lentiGuide vector (Addgene plasmid 52963), driven by a U6 promoter, was digested with BsmBI (NEB) and ligated with BsmBI-compatible annealed oligos (Supplementary table 2). An extra G was added to the 5' end of sgRNAs that lacked it to allow for U6 transcriptional initiation. Stable mutagenesis of endogenous *Calr* in Ba/F3 cells overexpressing Cas9 was achieved by lentiviral transduction of lentiGuide harboring sgRNA m1: 5'-GAGGACAAGAAGCGTAAAG-3'; sgRNA m2: 5'-AGGCTTAAGGAAGAAGAA-3' or a control scrambled vector. The lentiviral backbone vector and packaging plasmids were transfected into 293T cells and the viral supernatant was harvested 24 hours later. Parental Ba/F3 Cas9 cells and Ba/F3 Cas9 cells overexpressing hMPL, hEPOR or hG-CSFR were subjected to spin infection with viral supernatants, followed by 7 days of puromycin selection.

Sanger sequencing of Calr. CRISPR/Cas9 on-target gene editing of IL-3 independent Ba/F3-MPL-Cas9 cells was confirmed using Sanger sequencing following pGEM T-easy cloning of the PCR-amplified *Calr* exon 9 targeted region. First, genomic DNA was extracted (DNeasy Blood and Tissue Kit, Qiagen) from cells 8 days post-IL-3 withdrawal. PCR amplification of the *Calr* exon 9 locus was performed using 2x PCR Promega Master Mix (Thermo Fisher Scientific) and the following primers: Calr_Fwd (ACCACCTGTCTTTCCGTTCT) and Calr_Rev (GGCCTCTACAGCTCATCCTT) (IDT). The *Calr* PCR amplicons were ligated into a pGEM-T Easy vector using T4 DNA ligase (Promega) and incubated for 1 hour at room temperature. Transformation was carried out in JM109 competent cells and insert-containing white recombinant colonies were selected on LB agar plates containing X-gal and IPTG by incubating at 37°C overnight. The colonies were Sanger-sequenced using the universal primers T7 (TAATACGACTCACTATAGGG) and SP6 (ATTTAGGTGACACTATAG) to verify genome editing of the *Calr* exon 9 region.

Accession Number: Gene expression data is available in GEO database with the accession number GSE74890.

Intracellular Phosphoprotein Flow Cytometry Analysis. Ba/F3-MPL cells ectopically expressing CALR variants or Jak2V617F were cultured in RPMI with 10% FBS and 5% penicillin/streptomycin for 24 hours in the absence of mIL-3, followed by treatment with 1uM INCB018424 or DMSO for 3.5 hours. Harvested cells were fixed in 3-4% paraformaldehyde for 10 minutes, then permeabilized with ice-cold methanol for 10 minutes on ice or overnight at -20°C. Cells were washed twice in PBS with 1% BSA and staining was carried out in PBS 1% BSA for 30 min at 4°C with Alexa Fluor 647 Rabbit Anti pStat3 (Y705) (Cell Signaling Technology). Cells were washed after staining with PBS with 1% BSA and samples were analyzed using a FACS Canto cytometer (BD Biosciences). Data analysis was performed with FlowJo software V10.0.8.

Retroviral Bone Marrow Transplant. 6-8 week old C57BL/6 female mice were purchased Taconic (Hudson, NY). Retroviral supernatants were generated by transient co-transfection of 293T cells with MSCV-IRES-GFP empty vector, CALR WT or 52 bp deletion constructs and EcoPak packaging construct using TransIT LT-1 Reagent (Mirus Bio). Viral supernatant was collected 24 and 48 hours post-transfection. Two days before the BMT, bone marrow cells were collected from the femurs, tibias, and spines of donor mice. Cells were then incubated with CD117 (cKit) MicroBeads (Miltenyi Biotec) and subjected to positive selection using an autoMACS Pro Separator (Miltenyi Biotec). cKit enriched cells were then cultured overnight in SFEM medium supplemented with 50 ng/mL recombinant murine TPO, 50 ng/mL recombinant murine SCF, 10 ng/mL recombinant murine IL-3, and 10 ng/mL recombinant murine IL6. 18 hours later, cells

were infected with retroviral supernatant by spin infection on RetroNectin coated plates, and cultured overnight in SFEM media containing 50 ng/mL recombinant murine TPO, 50 ng/mL recombinant murine SCF, 10 ng/mL recombinant murine IL-3, and 10 ng/mL recombinant murine IL6. The following day, cells (1×10^6 per mouse) were resuspended in HBSS and injected retroorbitally into lethally irradiated (900 cGy) C57 BL/6 recipient mice. Peripheral blood was collected at indicated time points to monitor relative frequency of GFP positive cells. Following red blood cell lysis (BD Pharm Lyse; BD Biosciences) and homogenization through a 40-μm filter, samples were analyzed by flow cytometry using the fluorescence-activated cell sorter BD FACSCanto (BD Biosciences).

CBC Analysis. Mice were bled 0, 4 and 16 weeks post bone marrow transplant. 75 μL of blood was collected in EDTA capillary tubes and diluted with 300 μL PBS to produce a 1:5 dilution. Complete blood counts were run on the ADVIA 2120i blood analyzer (Siemens Healthcare Global, East Walpole, MA).

Stem and progenitor cell analysis. Bone marrow was collected and prepared for staining by red blood cell lysis (BD Pharmlyse, BD Biosciences) and homogenization through a 70micron filter. All samples were analyzed by flow cytometry using an LSR II (BD Biosciences). All staining steps were performed in ice-cold PBS containing 2% FBS. Post-acquisition analysis of data was performed with FlowJo software V9.2.3 (Treestar, CA). The following antibodies were used: lineage cocktail containing CD3ε (145-2C11), CD5 (53-7.3), Ter-119 (TER-119), Gr-1 (RB6-8C5), Mac-1 (M1/70) and B220 (30-F11); Kit (2B8), Sca-1 (D7), CD34 (Ram34), CD16/32 (93). For dead cell discrimination Dapi was used.

Histopathology. All mouse tissues were fixed in 10% neutral buffered formalin, embedded in paraffin, and stained with hematoxylin and eosin (H & E). Images of histological slides were obtained on a Nikon Eclipse E400 microscope (Nikon, Tokyo, Japan) equipped with a SPOT RT color digital camera model 2.1.1 (Diagnostic Instruments, Sterling Heights, MI). Bone marrow megakaryocytes were quantified by a pathologist, who was blinded to mouse genotype, and represent an average megakaryocyte count from 10 high-power fields assessed.

All human bone marrow biopsies were fixed overnight in Bouin solution (StatLab Medical Products, McKinney, TX) and decalcified for 15 minutes using RapidCal-Immuno (BBC Biochemical, Mt Vernon, Washington). Immunohistochemical studies were performed on paraffin sections using a recombinant rabbit monoclonal antibody to wild-type calreticulin (clone EPR3924, Abcam, Cambridge, MA). A synthetic peptide corresponding to residues in the N-terminal domain of calreticulin was used as an immuogen. Staining was performed on the Leica Bond III staining platform (dilution 1:2000) using the Bond Polymer Refine Detection kit (Leica Biosystems Inc, Buffalo Grove, IL). Antigen retrieval was performed using the Bond Epitope Retrieval 1 solution for 30 minutes.

Patient Studies. Immunohistochemical studies were performed on de-identified primary MPN bone marrow samples, under an IRB approved protocol (#2013P001110) at Brigham and Women's Hospital.

Statistical Analysis. All comparisons represent 2-tailed unpaired t-test analysis unless otherwise specified.

See supplementary information for:

Reagents, cell culture, RNA sequencing and statistical analyses for RNA sequencing.

ACKNOWLEDGEMENTS

This work was supported by the NIH (K08 HL109734 to AM), a Damon Runyon clinical investigator award (AM) and the Jeanne D. Housman Fund for Research on Myeloproliferative Disorders (AM). SE is a recipient of a T32 molecular hematology training award (NHLBI), EC is a recipient of a Lady Tata Memorial Trust Award, EAR is a recipient of an ASH Physician-Scientist Career Development Award and an ASH HONORS award. The authors thank Drs. Benjamin Ebert and Sagar Koduri and all members of the Mullally and Ebert laboratories for helpful discussions and input, and Professor Harvey Lodish (MIT) for his valuable insight and interest in our work.

Authorship Contributions: SE, NSA, EC, JAL and AM provided the concept, designed experiments and interpreted data. SE, NSA, EC, EAR, AK, FP, NF, SG performed experiments and analyzed data. ZT provided expertise and guidance for CRISPR/Cas9 experiments. OW provided primary MPN patient samples. JPP and FAS analyzed RNA sequencing data and performed GSEA analysis. EAM and RKS reviewed, interpreted and photographed immunohistochemistry and histopathology respectively. SE, NSA, EC and AM wrote the manuscript. All authors provided critical review of the manuscript.

REFERENCES

1. Campbell PJ, Green AR. The myeloproliferative disorders. N Engl J Med. 2006;355:2452-66.
2. Levine RL, Gilliland DG. Myeloproliferative disorders. Blood. 2008;112:2190-8.
3. Baxter EJ, Scott LM, Campbell PJ, East C, Fourouclas N, Swanton S, et al. Acquired mutation of the tyrosine kinase JAK2 in human myeloproliferative disorders. Lancet. 2005;365:1054-61.
4. James C, Ugo V, Le Couedic JP, Staerk J, Delhommeau F, Lacout C, et al. A unique clonal JAK2 mutation leading to constitutive signalling causes polycythaemia vera. Nature. 2005;434:1144-8.
5. Kralovics R, Passamonti F, Buser AS, Teo SS, Tiedt R, Passweg JR, et al. A gain-of-function mutation of JAK2 in myeloproliferative disorders. N Engl J Med. 2005;352:1779-90.
6. Levine RL, Wadleigh M, Cools J, Ebert BL, Wernig G, Huntly BJ, et al. Activating mutation in the tyrosine kinase JAK2 in polycythemia vera, essential thrombocythemia, and myeloid metaplasia with myelofibrosis. Cancer Cell. 2005;7:387-97.
7. Pikman Y, Lee BH, Mercher T, McDowell E, Ebert BL, Gozo M, et al. MPLW515L is a novel somatic activating mutation in myelofibrosis with myeloid metaplasia. PLoS medicine. 2006;3:e270.
8. Pardanani AD, Levine RL, Lasho T, Pikman Y, Mesa RA, Wadleigh M, et al. MPL515 mutations in myeloproliferative and other myeloid disorders: a study of 1182 patients. Blood. 2006;108:3472-6.
9. Oh ST, Simonds EF, Jones C, Hale MB, Goltsev Y, Gibbs KD, Jr., et al. Novel mutations in the inhibitory adaptor protein LNK drive JAK-STAT signaling in patients with myeloproliferative neoplasms. Blood. 2010;116:988-92.
10. Grand FH, Hidalgo-Curtis CE, Ernst T, Zoi K, Zoi C, McGuire C, et al. Frequent CBL mutations associated with 11q acquired uniparental disomy in myeloproliferative neoplasms. Blood. 2009;113:6182-92.
11. Sanada M, Suzuki T, Shih LY, Otsu M, Kato M, Yamazaki S, et al. Gain-of-function of mutated C-CBL tumour suppressor in myeloid neoplasms. Nature. 2009;460:904-8.
12. Vainchenker W, Delhommeau F, Constantinescu SN, Bernard OA. New mutations and pathogenesis of myeloproliferative neoplasms. Blood. 2011;118:1723-35.
13. Klampfl T, Gisslinger H, Harutyunyan AS, Nivarthi H, Rumi E, Milosevic JD, et al. Somatic mutations of calreticulin in myeloproliferative neoplasms. N Engl J Med. 2013;369:2379-90.
14. Nangalia J, Massie CE, Baxter EJ, Nice FL, Gundem G, Wedge DC, et al. Somatic CALR mutations in myeloproliferative neoplasms with nonmutated JAK2. N Engl J Med. 2013;369:2391-405.
15. Tannous A, Pisoni GB, Hebert DN, Molinari M. N-linked sugar-regulated protein folding and quality control in the ER. Semin Cell Dev Biol. 2015;41:79-89.
16. Michalak M, Corbett EF, Mesaeli N, Nakamura K, Opas M. Calreticulin: one protein, one gene, many functions. Biochem J. 1999;344 Pt 2:281-92.
17. Daley GQ, Van Etten RA, Baltimore D. Induction of chronic myelogenous leukemia in mice by the P210bcr/abl gene of the Philadelphia chromosome. Science. 1990;247:824-30.
18. Kelliher MA, McLaughlin J, Witte ON, Rosenberg N. Induction of a chronic myelogenous leukemia-like syndrome in mice with v-abl and BCR/ABL. Proc Natl Acad Sci U S A. 1990;87:6649-53.

19. Bumm TG, Elsea C, Corbin AS, Loriaux M, Sherbenou D, Wood L, et al. Characterization of murine JAK2V617F-positive myeloproliferative disease. Cancer research. 2006;66:11156-65.
20. Lacout C, Pisani DF, Tulliez M, Gachelin FM, Vainchenker W, Villeval JL. JAK2V617F expression in murine hematopoietic cells leads to MPD mimicking human PV with secondary myelofibrosis. Blood. 2006;108:1652-60.
21. Wernig G, Mercher T, Okabe R, Levine RL, Lee BH, Gilliland DG. Expression of Jak2V617F causes a polycythemia vera-like disease with associated myelofibrosis in a murine bone marrow transplant model. Blood. 2006;107:4274-81.
22. Zaleskas VM, Krause DS, Lazarides K, Patel N, Hu Y, Li S, et al. Molecular pathogenesis and therapy of polycythemia induced in mice by JAK2 V617F. PloS one. 2006;1:e18.
23. Mullally A, Lane SW, Brumme K, Ebert BL. Myeloproliferative neoplasm animal models. Hematology/oncology clinics of North America. 2012;26:1065-81.
24. Vannucchi AM, Rotunno G, Bartalucci N, Raugei G, Carrai V, Balliu M, et al. Calreticulin mutation-specific immunostaining in myeloproliferative neoplasms: pathogenetic insight and diagnostic value. Leukemia. 2014;28:1811-8.
25. Stein H, Bob R, Durkop H, Erck C, Kampfe D, Kvasnicka HM, et al. A new monoclonal antibody (CAL2) detects CALRETICULIN mutations in formalin-fixed and paraffin-embedded bone marrow biopsies. Leukemia. 2016;30:131-5.
26. Daley GQ, Baltimore D. Transformation of an interleukin 3-dependent hematopoietic cell line by the chronic myelogenous leukemia-specific P210bcr/abl protein. Proc Natl Acad Sci U S A. 1988;85:9312-6.
27. Lu X, Levine R, Tong W, Wernig G, Pikman Y, Zarnegar S, et al. Expression of a homodimeric type I cytokine receptor is required for JAK2V617F-mediated transformation. Proc Natl Acad Sci U S A. 2005;102:18962-7.
28. Komatsu N, Nakauchi H, Miwa A, Ishihara T, Eguchi M, Moroi M, et al. Establishment and characterization of a human leukemic cell line with megakaryocytic features: dependency on granulocyte-macrophage colony-stimulating factor, interleukin 3, or erythropoietin for growth and survival. Cancer research. 1991;51:341-8.
29. Doench JG, Hartenian E, Graham DB, Tothova Z, Hegde M, Smith I, et al. Rational design of highly active sgRNAs for CRISPR-Cas9-mediated gene inactivation. Nature biotechnology. 2014;32:1262-7.
30. Basham B, Sathe M, Grein J, McClanahan T, D'Andrea A, Lees E, et al. In vivo identification of novel STAT5 target genes. Nucleic Acids Res. 2008;36:3802-18.
31. Baker SJ, Rane SG, Reddy EP. Hematopoietic cytokine receptor signaling. Oncogene. 2007;26:6724-37.
32. Azare J, Leslie K, Al-Ahmadie H, Gerald W, Weinreb PH, Violette SM, et al. Constitutively activated Stat3 induces tumorigenesis and enhances cell motility of prostate epithelial cells through integrin beta 6. Molecular and cellular biology. 2007;27:4444-53.
33. Verstovsek S, Kantarjian H, Mesa RA, Pardanani AD, Cortes-Franco J, Thomas DA, et al. Safety and efficacy of INCB018424, a JAK1 and JAK2 inhibitor, in myelofibrosis. N Engl J Med. 2010;363:1117-27.
34. Moremen KW, Molinari M. N-linked glycan recognition and processing: the molecular basis of endoplasmic reticulum quality control. Current opinion in structural biology. 2006;16:592-9.
35. Marty C, Pecquet C, Nivarthi H, Elkhoury M, Chachoua I, Tulliez M, et al. Calreticulin mutants in mice induce an MPL-dependent thrombocytosis with frequent progression to myelofibrosis. Blood. 2015.

36. Chachoua I, Pecquet C, El-Khoury M, Nivarthi H, Albu RI, Marty C, et al. Thrombopoietin receptor activation by myeloproliferative neoplasm associated calreticulin mutants. Blood. 2015.
37. Wernig G, Gonneville JR, Crowley BJ, Rodrigues MS, Reddy MM, Hudon HE, et al. The Jak2V617F oncogene associated with myeloproliferative diseases requires a functional FERM domain for transformation and for expression of the Myc and Pim proto-oncogenes. Blood. 2008;111:3751-9.
38. Rumi E, Pietra D, Ferretti V, Klampfl T, Harutyunyan AS, Milosevic JD, et al. JAK2 or CALR mutation status defines subtypes of essential thrombocythemia with substantially different clinical course and outcomes. Blood. 2014;123:1544-51.
39. Rumi E, Pietra D, Pascutto C, Guglielmelli P, Martinez-Trillos A, Casetti I, et al. Clinical effect of driver mutations of JAK2, CALR, or MPL in primary myelofibrosis. Blood. 2014;124:1062-9.
40. Rampal R, Al-Shahrour F, Abdel-Wahab O, Patel JP, Brunel JP, Mermel CH, et al. Integrated genomic analysis illustrates the central role of JAK-STAT pathway activation in myeloproliferative neoplasm pathogenesis. Blood. 2014;123:e123-33.
41. Passamonti F, Caramazza D, Maffioli M. JAK inhibitor in CALR-mutant myelofibrosis. N Engl J Med. 2014;370:1168-9.
42. Chen E, Mullally A. How does JAK2V617F contribute to the pathogenesis of myeloproliferative neoplasms? Hematology / the Education Program of the American Society of Hematology American Society of Hematology Education Program. 2014;2014:268-76.
43. Moraga I, Wernig G, Wilmes S, Gryshkova V, Richter CP, Hong WJ, et al. Tuning cytokine receptor signaling by re-orienting dimer geometry with surrogate ligands. Cell. 2015;160:1196-208.
44. Pietra D, Rumi E, Ferretti VV, Di Buduo CA, Milanesi C, Cavalloni C, et al. Differential clinical effects of different mutation subtypes in CALR-mutant myeloproliferative neoplasms. Leukemia. 2015.

FIGURE LEGENDS

Figure 1. Mutant CALR is sufficient to engender an MPN phenotype in mice

(A) Retroviral bone marrow transplant (BMT) scheme. (B) White blood cell (WBC) count, hematocrit (HCT), platelet count (PLT) at 16 weeks post-transplantation in peripheral blood (PB) of recipient mice receiving empty vector (EV), wild-type CALR ($CALR^{WT}$) or mutant CALR ($CALR^{MUT}$)-expressing c-Kit+ bone marrow (BM) cells (mean ± SD, n=5 in each group) demonstrates significant thrombocytosis in $CALR^{MUT}$ group (C) Histopathologic H&E sections of BM from representative EV, $CALR^{WT}$ or $CALR^{MUT}$ recipient mice demonstrates macro-megakaryocytes, megakaryocytes with hyper-lobated nuclei, megakaryocytic clustering, emperipolesis, and atypical location at sinusoids and trabecular bone in $CALR^{MUT}$ recipient animals (20X magnification) (D) Megakaryocyte counts per high power field (HPF) in BM of EV, $CALR^{WT}$ or $CALR^{MUT}$ recipient mice demonstrates increased megakaryocyte number in $CALR^{MUT}$ recipient animals.

All p values were determined by unpaired two-tailed Student's t test (*$0.01 < p < 0.05$; **$0.001 < p < 0.01$; ns, not significant).

Figure 2. MPL is required for mutant CALR-mediated cellular transformation

(A – D) Growth curves in parental Ba/F3 cells (A), Ba/F3-MPL cells (B), Ba/F3-EPOR cells (C), and Ba/F3-G-CSFR cells (D) stably expressing EV, $CALR^{WT}$, $CALR^{MUT}$, or Jak2V617F demonstrate IL-3 independent growth in $CALR^{MUT}$-expressing Ba/F3-MPL cells but not in parental Ba/F3, Ba/F3-EPOR or Ba/F3-G-CSFR cells. (E – G) Growth curve in parental UT-7 (E), UT-7-MPL (F), or UT-7-EPOR (G) cells ectopically expressing CALR variants demonstrates GM-CSF-independent growth in $CALR^{MUT}$-expressing UT-7-MPL cells only.

Figure 3. Introduction of +1 bp frameshift mutations into the endogenous *Calr* locus is sufficient to confer oncogenic activity to Calr

(A – D) Growth curves in parental Ba/F3-Cas9 cells (A) Ba/F3-MPL-Cas9 cells (B), Ba/F3-EPOR-Cas9 cells (C), and Ba/F3-G-CSFR-Cas9 cells (D) demonstrates IL-3 independent growth in *Calr*-targeted Ba/F3-MPL-Cas9 cells only (E) Sequence verification confirming on-target editing of endogenous *Calr* (exon 9) in Ba/F3-MPL cells. +1 bp frameshift mutations are indicated in black.

Figure 4. Mutant CALR activates the JAK-STAT signaling axis downstream of MPL

(A) Pre-ranked GSEA in $CALR^{MUT}$ versus $CALR^{WT}$ expressing Ba/F3-MPL cells 24 hours post-IL-3 withdrawal. Stat5 target genes are enriched in $CALR^{MUT}$ compared to $CALR^{WT}$-expressing Ba/F3-MPL cells (left) and Stat3 target genes are enriched in $CALR^{MUT}$ compared to $CALR^{WT}$-expressing Ba/F3-MPL cells (right) (B) Immunoblotting demonstrates differential phosphorylation of MPL and Jak2 in Ba/F3-MPL transformed by $CALR^{MUT}$ (C) Immunoblotting demonstrates differential phosphorylation of Stat5 and Stat3 in Ba/F3-MPL cells transformed by $CALR^{MUT}$, but not in parental Ba/F3, Ba/F3-EPOR, or Ba/F3-G-CSFR cells stably expressing $CALR^{MUT}$.

Figure 5. Mutant CALR-transformed hematopoietic cells are sensitive to JAK2 inhibition

(A) Growth curve in $CALR^{MUT}$-transformed Ba/F3-MPL cells transduced with shRNAs targeting Jak2 (shJak2 #1 or shJak2 #2) or a non-targeting shRNA control (shLuc) demonstrates significantly decreased proliferation in cells subjected to Jak2 knockdown compared to control cells (B) Intracellular phosphoprotein flow cytometry analysis of $CALR^{MUT}$ (left) or Jak2V617F (right) expressing-Ba/F3-MPL cells demonstrates

abrogation of Stat3 phosphorylation in response to treatment with the JAK2 inhibitor, INCB018424. (C) Pre-ranked GSEA in $CALR^{MUT}$ versus $CALR^{WT}$ expressing Ba/F3-MPL cells 24 hours post-IL-3 withdrawal performed on a consensus signature of genes downregulated by JAK2 inhibitor ruxolitinib (2μM dose, 6 hours). Individual perturbational signatures (the top 100 most downregulated) for each assay (6 different cancer cell lines in total) were obtained by using the Lincscloud API (version a2, LINCS Production Phase L1000 data, Broad Institute) from the NIH LINCS Program resource. For the consensus signature, only genes from the top 100 present in at least two assays were considered for further analysis.

All p values were determined by unpaired two-tailed Student's t test (*$0.01 < p < 0.05$; (**$0.001 < p < 0.01$; ns, not significant)

Figure 6. Structure-function analysis of mutant CALR uncovers a critical oncogenic role for the positive electrostatic charge of the mutant C-terminus

(A) Schema of domain and sequence mutants generated from $CALR^{WT}$ and $CALR^{MUT}$. (B) Growth curve in Ba/F3-MPL cells stably expressing CALR domain mutants demonstrates that the mutant C-terminus alone is insufficient for transformation. (C). Growth curve in Ba/F3-MPL cells stably expressing CALRΔKDEL mutant demonstrates that deleting the KDEL from $CALR^{WT}$ is insufficient for transformation. (D) Growth curve in Ba/F3-MPL cells stably expressing $CALR^{MUT}$ C-terminus sequence-mutants demonstrates that all transform Ba/F3-MPL cells with equal efficacy. (E) (Top) Scheme of $CALR^{MUT}$-neutral and $CALR^{MUT}$-positive charge mutants. (Bottom) Growth curve in Ba/F3-MPL cells stably expressing $CALR^{MUT}$-neutral or $CALR^{MUT}$-positive variants shows that loss of the net positive charge in the mutant C-terminus abolishes the transforming capacity of $CALR^{MUT}$.

Figure 7. Mutant CALR binds to MPL and this interaction correlates with the transforming capacity of mutant CALR

(A - C) Immunoblotting of FLAG-immunoprecipitated proteins and whole cell lysates from 293T cells co-transfected with FLAG-CALR variants and (A) MPL, (B) EPOR or (C) G-CSFR demonstrates that $CALR^{MUT}$ differentially binds to MPL, but not to other type I cytokine receptors (D) Immunoblotting of GST-immunoprecipitated proteins and whole cell lysates from 293T cells co-transfected with GST-CALR domain mutants and MPL demonstrates that only full length $CALR^{MUT}$, and not the mutant C-terminus alone, binds to MPL (E) Immunoblotting of FLAG-immunoprecipitated proteins and whole cell lysates from 293T cells co-transfected with mutant FLAG-$CALR^{MUT}$ charge variants and MPL demonstrates that $CALR^{MUT}$-neutral binding to MPL is markedly diminished compared to $CALR^{MUT}$-positive or $CALR^{MUT}$ binding.

Figure 1

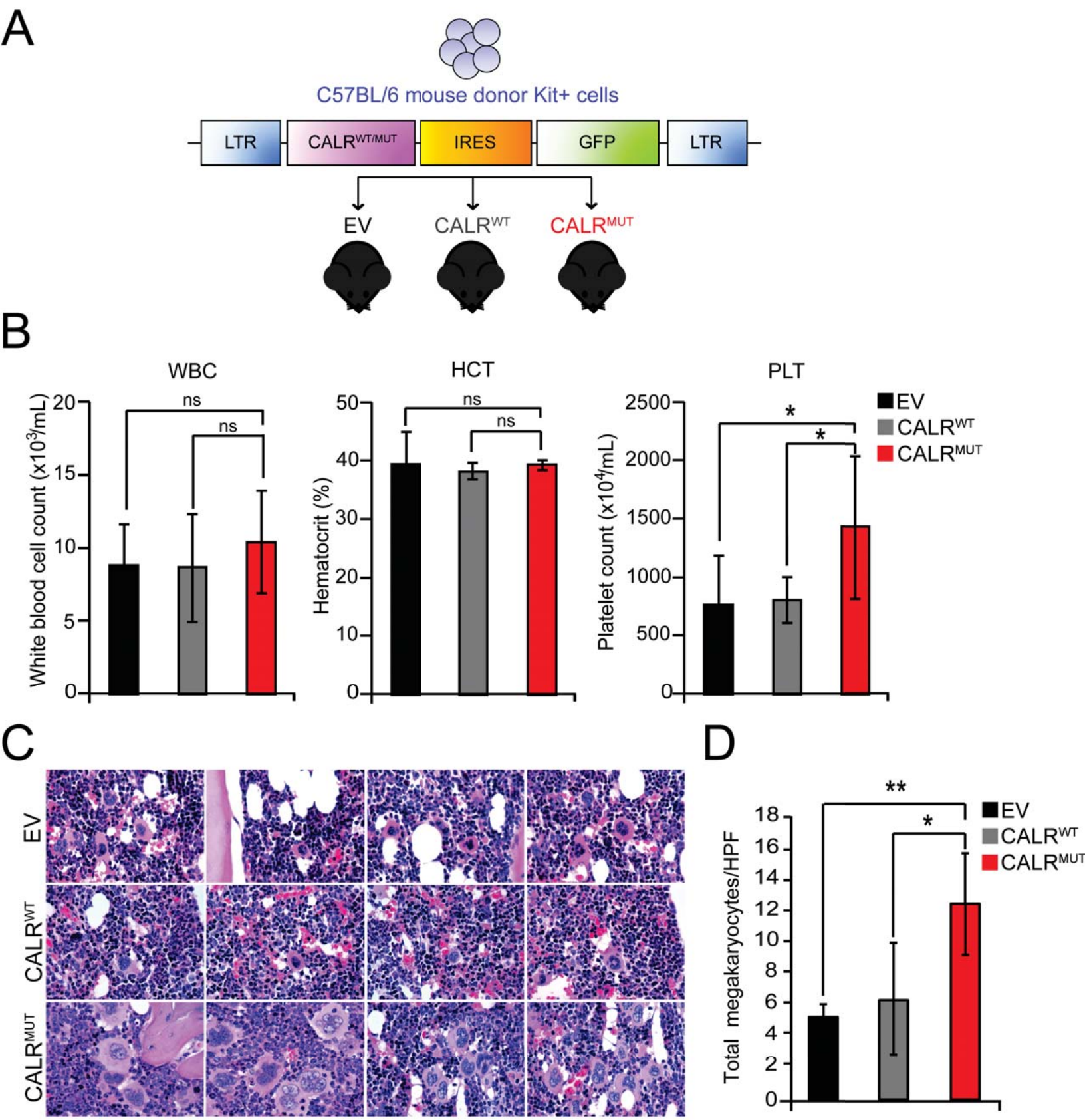
A
C57BL/6 mouse donor Kit+ cells
LTR
CALR^WT/MUT
IRES
GFP
LTR
EV
CALR^WT
CALR^MUT
B
WBC
White blood cell count (x10^3/mL)
ns
ns
HCT
Hematocrit (%)
ns
ns
PLT
Platelet count (x10^4/mL)
*
*
EV
CALR^WT
CALR^MUT
C
EV
CALR^WT
CALR^MUT
D
Total megakaryocytes/HPF
**
*
EV
CALR^WT
CALR^MUT

Figure 2

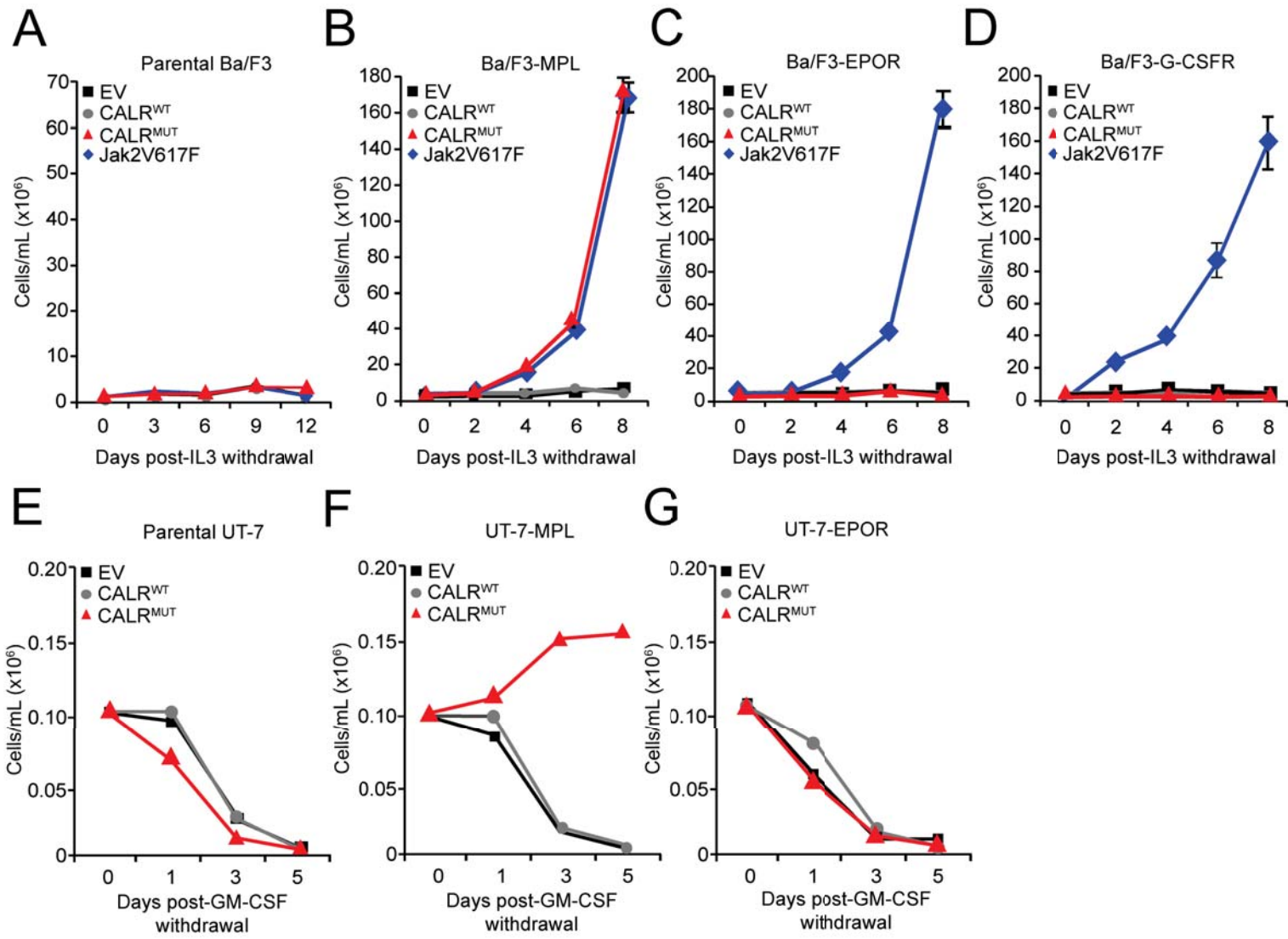
A
Parental Ba/F3
EV
CALR^WT
CALR^MUT
Jak2V617F
Cells/mL (x10^6)
Days post-IL3 withdrawal
B
Ba/F3-MPL
C
Ba/F3-EPOR
D
Ba/F3-G-CSFR
E
Parental UT-7
F
UT-7-MPL
G
UT-7-EPOR
Days post-GM-CSF withdrawal

Figure 3

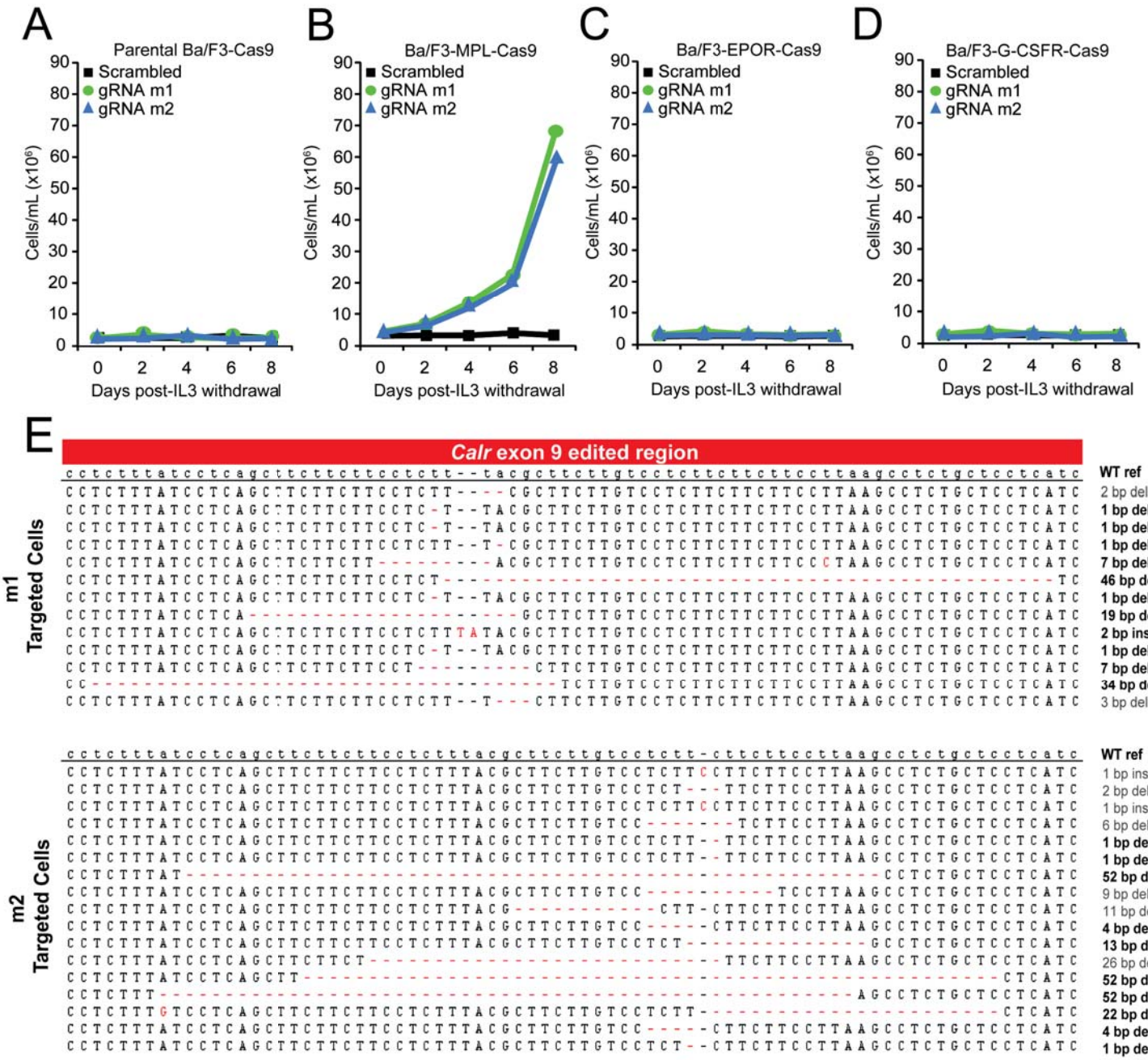
A
Parental Ba/F3-Cas9
B
Ba/F3-MPL-Cas9
C
Ba/F3-EPOR-Cas9
D
Ba/F3-G-CSFR-Cas9
Scrambled
gRNA m1
gRNA m2
Cells/mL (x10⁶)
Days post-IL3 withdrawal
E
Calr exon 9 edited region
m1 Targeted Cells
m2 Targeted Cells
WT ref
2 bp del
1 bp del
7 bp del
46 bp del
19 bp del
2 bp ins
34 bp del
3 bp del
1 bp ins
6 bp del
52 bp del
9 bp del
11 bp del
4 bp del
13 bp del
26 bp del
22 bp del

Figure 4

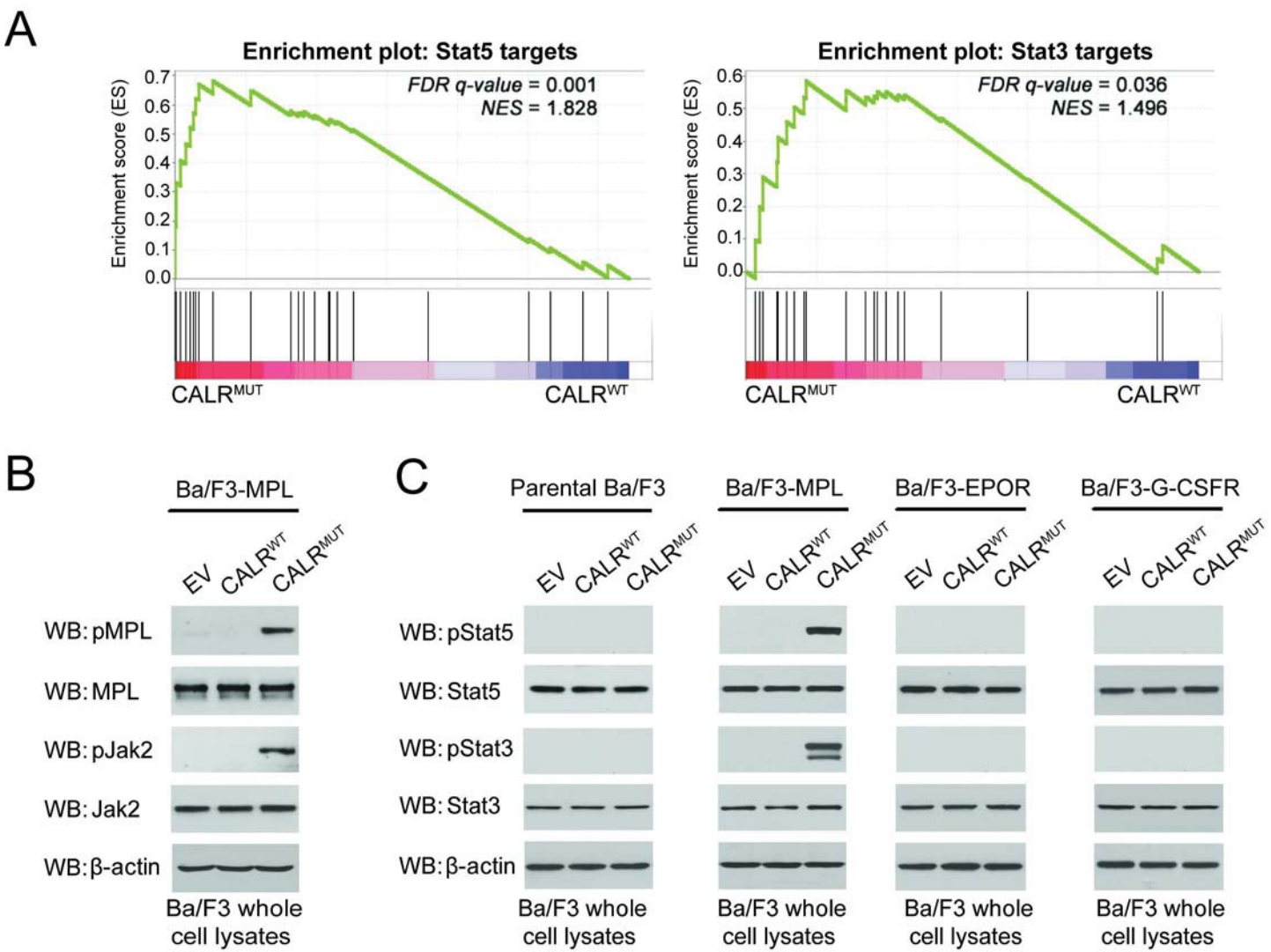
A
Enrichment plot: Stat5 targets
FDR q-value = 0.001
NES = 1.828
Enrichment score (ES)
CALRMUT
CALRWT
Enrichment plot: Stat3 targets
FDR q-value = 0.036
NES = 1.496
Enrichment score (ES)
CALRMUT
CALRWT
B
Ba/F3-MPL
EV
CALRWT
CALRMUT
WB: pMPL
WB: MPL
WB: pJak2
WB: Jak2
WB: β-actin
Ba/F3 whole cell lysates
C
Parental Ba/F3
Ba/F3-MPL
Ba/F3-EPOR
Ba/F3-G-CSFR
EV
CALRWT
CALRMUT
WB: pStat5
WB: Stat5
WB: pStat3
WB: Stat3
WB: β-actin
Ba/F3 whole cell lysates

Figure 5

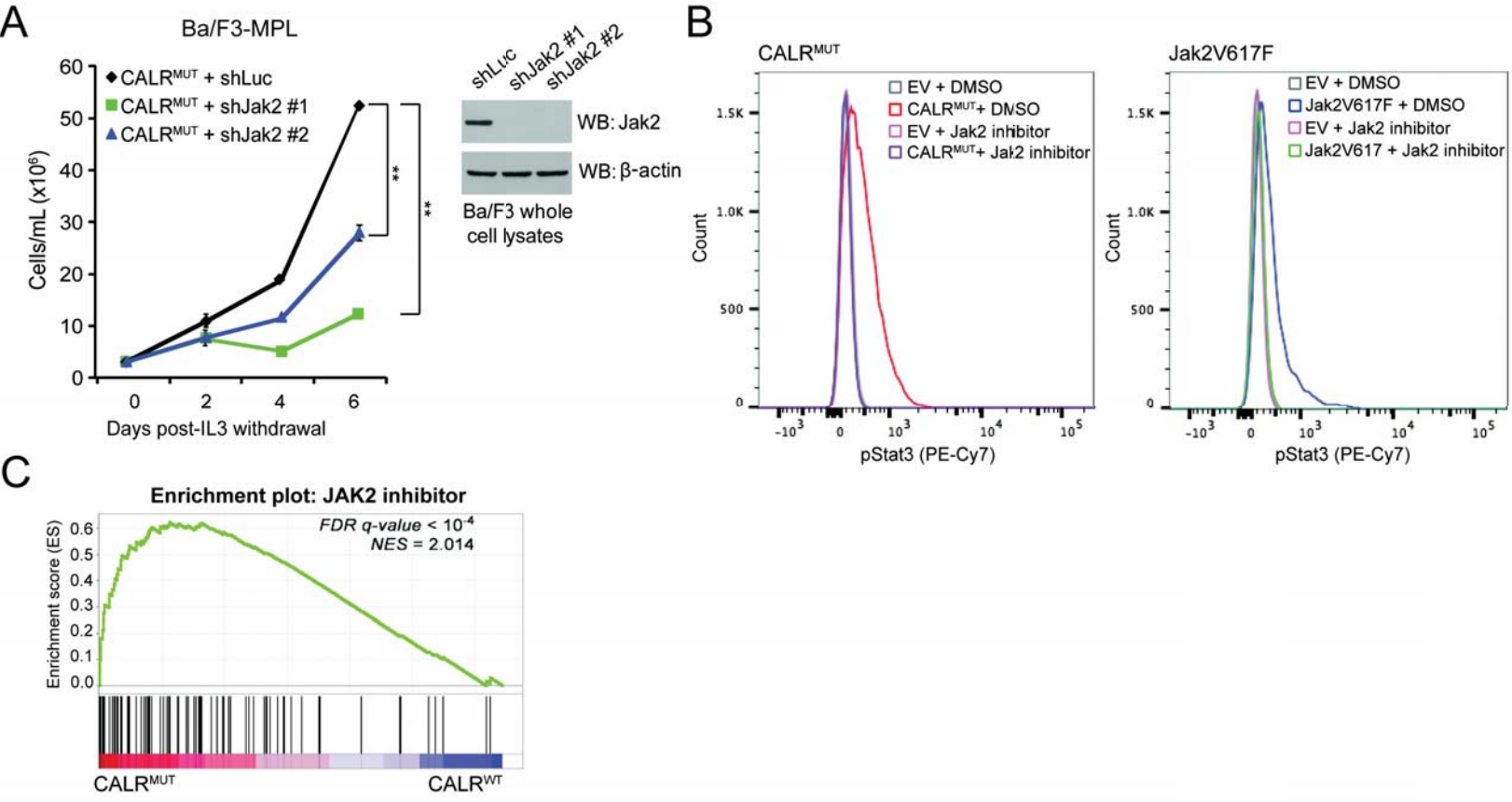
A
Ba/F3-MPL
CALR^MUT + shLuc
CALR^MUT + shJak2 #1
CALR^MUT + shJak2 #2
Cells/mL (x10^6)
Days post-IL3 withdrawal
**
**
shLuc
shJak2 #1
shJak2 #2
WB: Jak2
WB: β-actin
Ba/F3 whole cell lysates
B
CALR^MUT
EV + DMSO
CALR^MUT + DMSO
EV + Jak2 inhibitor
CALR^MUT + Jak2 inhibitor
Count
pStat3 (PE-Cy7)
Jak2V617F
EV + DMSO
Jak2V617F + DMSO
EV + Jak2 inhibitor
Jak2V617 + Jak2 inhibitor
Count
pStat3 (PE-Cy7)
C
Enrichment plot: JAK2 inhibitor
FDR q-value < 10^-4
NES = 2.014
Enrichment score (ES)
CALR^MUT
CALR^WT

Figure 6

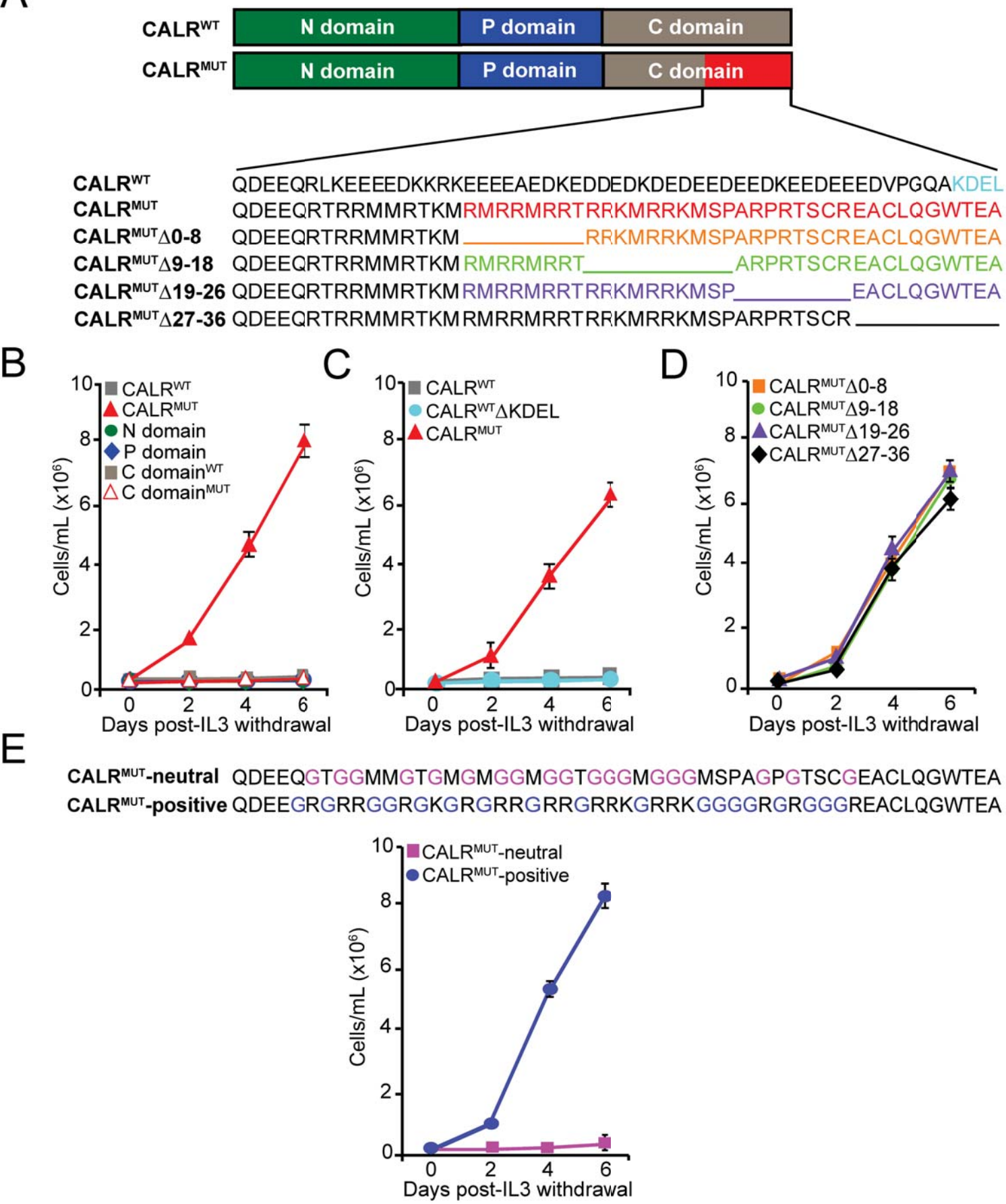
A
CALR^WT
N domain
P domain
C domain
CALR^MUT
N domain
P domain
C domain
CALR^WT QDEEQRLKEEEEDKKRKEEEEAEDKEDDEDKDEDEEDEEDKEEDEEEDVPGQAKDEL
CALR^MUT QDEEQRTRRMMRTKMRMRRMRRTRRKMRRKMSPARPRTSCREACLQGWTEA
CALR^MUTΔ0-8 QDEEQRTRRMMRTKM RRKMRRKMSPARPRTSCREACLQGWTEA
CALR^MUTΔ9-18 QDEEQRTRRMMRTKMRMRRMRRT ARPRTSCREACLQGWTEA
CALR^MUTΔ19-26 QDEEQRTRRMMRTKMRMRRMRRTRRKMRRKMSP EACLQGWTEA
CALR^MUTΔ27-36 QDEEQRTRRMMRTKMRMRRMRRTRRKMRRKMSPARPRTSCR
B
CALR^WT
CALR^MUT
N domain
P domain
C domain^WT
C domain^MUT
Cells/mL (x10^6)
Days post-IL3 withdrawal
C
CALR^WT
CALR^WTΔKDEL
CALR^MUT
Cells/mL (x10^6)
Days post-IL3 withdrawal
D
CALR^MUTΔ0-8
CALR^MUTΔ9-18
CALR^MUTΔ19-26
CALR^MUTΔ27-36
Cells/mL (x10^6)
Days post-IL3 withdrawal
E
CALR^MUT-neutral QDEEQGTGGMMGTGMGMGGMGGTGGGMGGGMSPAGPGTSCGEACLQGWTEA
CALR^MUT-positive QDEEGRGRRGGRGKGRGRRGRRGRRKGRRKGGGGRGRGGGREACLQGWTEA
CALR^MUT-neutral
CALR^MUT-positive
Cells/mL (x10^6)
Days post-IL3 withdrawal

Figure 7

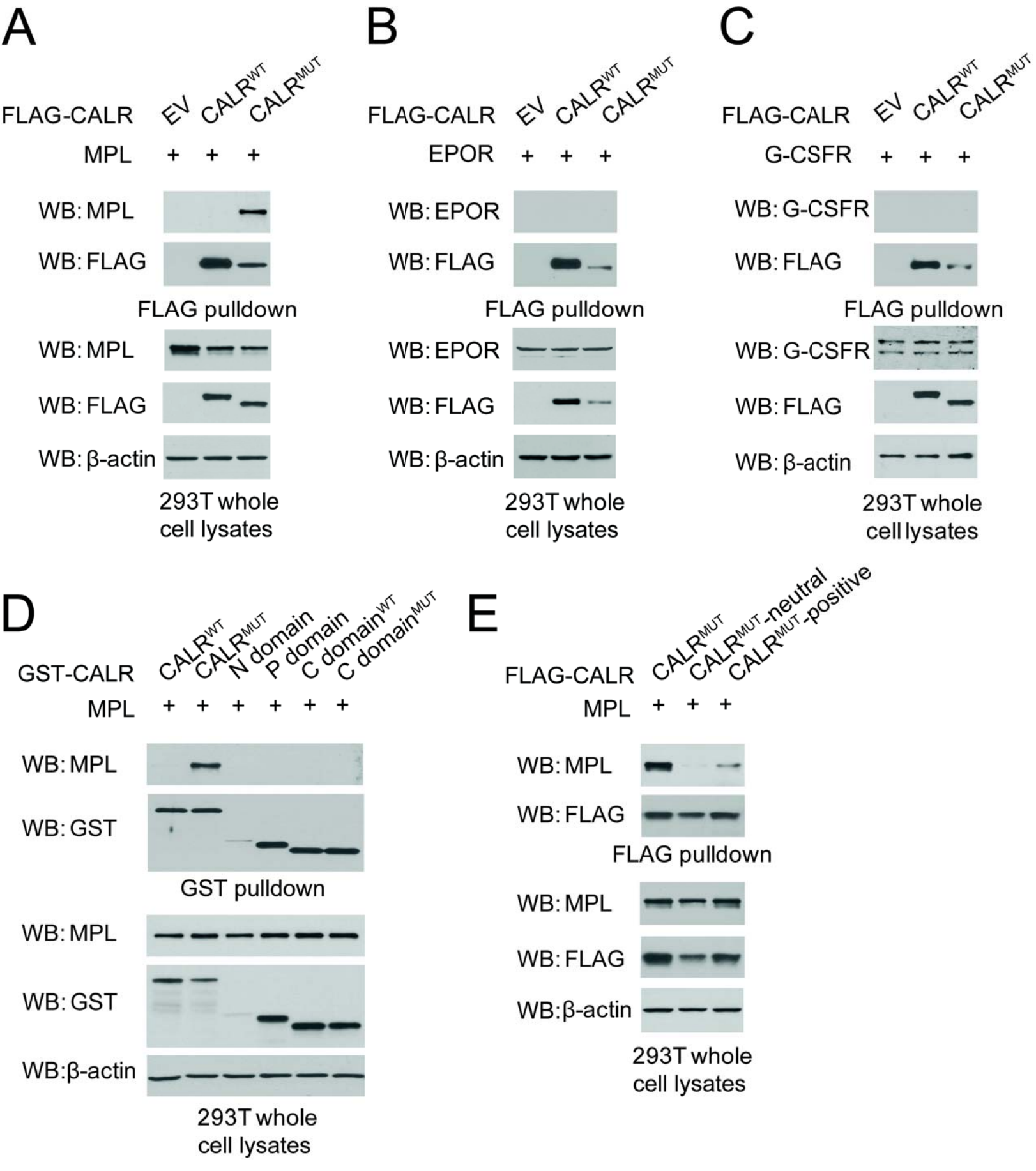
A
FLAG-CALR
EV
CALRWT
CALRMUT
MPL + + +
WB: MPL
WB: FLAG
FLAG pulldown
WB: MPL
WB: FLAG
WB: β-actin
293T whole cell lysates
B
FLAG-CALR
EV
CALRWT
CALRMUT
EPOR + + +
WB: EPOR
WB: FLAG
FLAG pulldown
WB: EPOR
WB: FLAG
WB: β-actin
293T whole cell lysates
C
FLAG-CALR
EV
CALRWT
CALRMUT
G-CSFR + + +
WB: G-CSFR
WB: FLAG
FLAG pulldown
WB: G-CSFR
WB: FLAG
WB: β-actin
293T whole cell lysates
D
GST-CALR
CALRWT
CALRMUT
N domain
P domain
C domainWT
C domainMUT
MPL + + + + + +
WB: MPL
WB: GST
GST pulldown
WB: MPL
WB: GST
WB:β-actin
293T whole cell lysates
E
FLAG-CALR
CALRMUT
CALRMUT-neutral
CALRMUT-positive
MPL + + +
WB: MPL
WB: FLAG
FLAG pulldown
WB: MPL
WB: FLAG
WB:β-actin
293T whole cell lysates